The Astrophysical Journal, 729:79 (8pp), 2011 March 10 doi:10.1088/0004-637X/729/2/79

DIFFERENTIAL ROTATION OF THE ULTRAVIOLET CORONA AT SOLAR MAXIMUM

Salvatore Mancuso and Silvio Giordano
Istituto Nazionale di Astrofisica (INAF), Osservatorio Astronomico di Torino, Strada Osservatorio 20, 10025 Pino Torinese (To), Italy; mancuso@oato.inaf.it
Received 2010 June 23; accepted 2010 December 23; published 2011 February 11

ABSTRACT

Synoptic observations of the O VI 1032 Å spectral line from the UltraViolet Coronagraph Spectrometer (UVCS) telescope on board the *Solar and Heliospheric Observatory* (*SOHO*) have been analyzed in order to establish the rotational characteristics of the solar corona in the time interval from 1999 March 18 to 2002 December 31, corresponding to the maximum phase of solar cycle 23. By using autocorrelation analysis techniques, we determined the latitude and time dependence of the coronal rotation rate at a heliocentric distance of 1.6 $R_\odot$ from the solar equator up to about 15° from the poles. Although the equatorial rotation rate is initially consistent with the coronal synodic rotation period (∼27.5 days) inferred in a previous study by Giordano & Mancuso around solar minimum, a systematic and substantial acceleration is observed to occur during the second part of the year 2000, with the equatorial coronal synodic rotation period settling to an average value of 25.7 days in the time interval extending from 2001 August to 2002 April, corresponding to a ∼7% increase in coronal rotation rate. It is shown that the coronal magnetic structures rotate much faster at all latitudes, and less differentially, than the underlying small-scale magnetic structures linked to the photospheric plasma. The rotation rate of sunspots is however compatible, at least within ∼20° from the solar equator, with the one estimated in the middle corona.

Key words: Sun: corona – Sun: rotation – Sun: UV radiation

1. INTRODUCTION

The variation in rotation rate with latitude of the solar corona, an effect known as coronal differential rotation, remains as yet a poorly understood and debated topic. In fact, the determination of rotation rates is not a simple task as it depends sensibly upon both the methods applied and the type of data being used, each technique having its own difficulties and uncertainties. Previous studies of coronal rotation were mainly based on observations obtained in white light (Hansen et al. 1969; Fisher & Sime 1984; Nash 1991; Lewis et al. 1999; Lewis & Simnett 2001), Fe XIV 5303 Å green line (Sime et al. 1989; Wang et al. 1997; Altrock 2003), microwaves (Aschwanden et al. 1995), soft X-rays (Timothy et al. 1975; Weber et al. 1999), or extrapolation of photospheric data (Hoeksema & Scherrer 1987; Wang et al. 1988). Like the underlying photosphere, the corona was observed to rotate faster near the equator and to slow down its rate with latitude toward the poles. Direct comparison with photospheric rotation is however complicated by the fact that the corona is optically thin across a wide range of wavelengths and thus subject to important line-of-sight effects. Moreover, the observed coronal features are, in general, far less distinct both in duration and in extent than the photospheric tracers.

Studies of the variation of the coronal differential rotation with time are further suggestive of solar-cycle variations in the latitude-dependent rotation linked to the increase in solar activity and the consequent emergence of magnetic flux associated with bipolar regions, with activity speeding up the rotation rate (e.g., Mouradian et al. 2002). Sime et al. (1989) and Altrock (2003), from their analyses of synoptic observations of the green coronal line, reported a weak, solar-cycle-dependent differential rotation, pointing out that the corona shows rigid rotation near solar minimum and differential rotation near solar maximum. On the other hand, from observations of the green solar corona, Rybak (1994) did not find a clear signature of cyclic variation of the rotation over the epoch from 1964 to 1989, while Tlatov (2006), using similar measurements from a wider time interval (1939–2004), claimed that deceleration of the rotational velocity of the corona at low and middle latitudes occurs at activity maxima. Clearly, the long-term variation in the rotation of the solar corona is not well understood as yet.

In the corona, the determination of the differential rotation rate is usually obtained indirectly because of the occurrence, at various latitudes, of localized and bright coronal structures associated with streamers having sufficient stability to reappear, after at least one rotation, at the same limb. Of course, coronal features change size and shape and may even move above the solar surface on order of days. They might thus be hardly re-identifiable even after just one rotation, although previous studies clearly indicate that these structures are actually able to persist for several rotations. At solar minimum, there are in general only a few of these tracers, so that the calculation of the differential rotation of the corona is quite straightforward. During solar maximum conditions, however, the presence of transient events, the consecutive or even simultaneous emergence, growth, and decay of several active regions randomly distributed over longitude and latitude, and the suspected time-dependent evolution of the rotation rate at different latitudes has the potential to undermine the possibility of a clear detection of a unique periodicity along a selected latitude, especially when the available temporal and angular resolutions are not high enough. Moreover, projection effects due to coronal features rooted at lower latitudes and to streamers out of the plane of the sky could complicate the analysis even further. For the above reasons, observations of coronal rotation during increased solar activity pose, in general, several difficulties in both their analysis and interpretation.

This work follows a previous study (Giordano & Mancuso 2008, hereafter Paper I) on the rotation of the solar corona as obtained through the analysis of the intensity time series of the O VI 1032 Å spectral line, routinely observed by the UltraViolet Coronagraph Spectrometer (UVCS; Kohl et al. 1995) telescope on board the *Solar and Heliospheric Observatory* (*SOHO*; Domingo et al. 1995) spacecraft. Compared to other tracers of solar activity, such as sunspots or active regions, coronal spectral

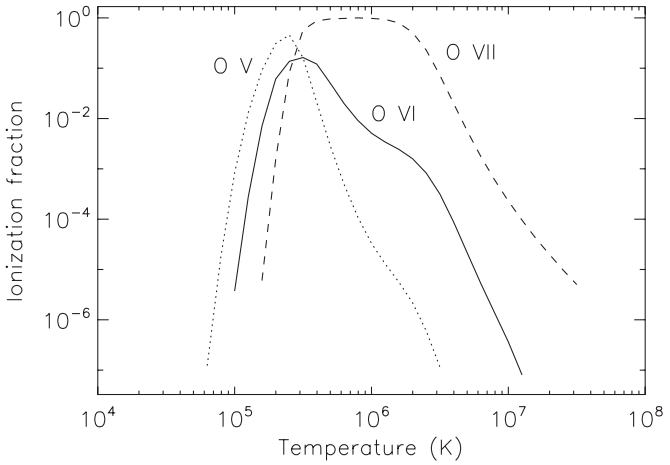

Figure 1. Ionization fraction curves as a function of temperature for three different oxygen ions. From Giordano (1998).

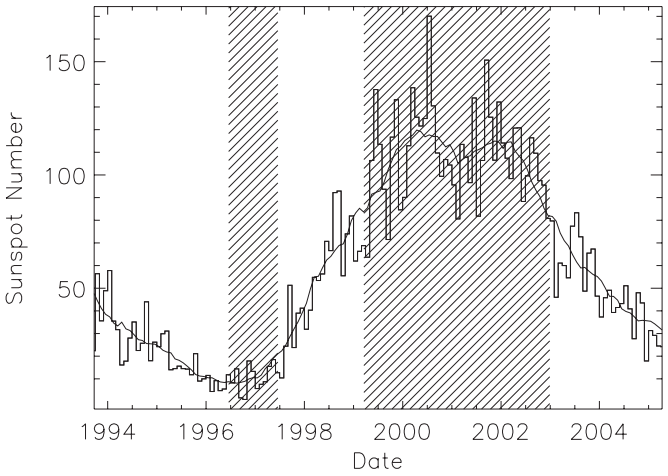

Figure 2. Monthly and monthly smoothed sunspot numbers from 1994 to 2005. The shaded regions show the two different time intervals that have been used for the study of the coronal rotation at solar minimum (Paper I) and at solar maximum (this work). Courtesy of Solar Influences Data Analysis Center (SIDC), Belgium.

lines have the advantage of being detectable over a wide range of latitudes from the solar equator up to the poles. The extensive database acquired by UVCS extends to an entire solar cycle and contains a wealth of information about the dependence of the coronal rotation rate on time, latitude, and height. At solar minimum, Giordano & Mancuso (2008) confirmed results from previous investigations, showing that the solar corona rotates less differentially than the underlying photosphere. In that work, the mean coronal synodic equatorial rotation period (the apparent rotation period as seen from the Earth) of the corona was estimated at 27.5 ± 0.1 days. From the analysis of the variation of the coronal rotation with latitude, the UV corona was seen to increase its rotation period from the equator up to the poleward boundary of the mid-latitude streamers, reaching a peak of 28.2 ± 0.2 days around 120° in the southern quadrant and a peak of 27.6 ± 0.2 days around 60° in the northern quadrant. While the study in Paper I was based on the analysis of the coronal rotation period over a one-year interval during solar minimum conditions, the present work extends the periodicity analysis to a wider time range covering the full solar maximum phase of cycle 23.

The paper is structured as follows. In Section 2, we present the observations and the data reduction techniques. In Section 3, we give a description of the autocorrelation methods applied to retrieve periodicities from the time series analysis. In Section 4, we outline the different steps in our analysis and present our results. Finally, we summarize our conclusions in Section 5.

2. OBSERVATIONS AND DATA REDUCTION

The data used in this work were collected during regular observations of the coronal O VI 1032 Å spectral line, routinely observed by UVCS/*SOHO*. The UVCS instrument is an internally and externally occulted coronagraph consisting of two spectrometric channels for the observation of spectral lines in the UV range and a visible light channel for polarimetric measurements of the extended solar corona. The UVCS slit, parallel to a tangent to the solar limb on the plane of the sky, can be moved along the radial direction and is therefore able to yield raster observations of the solar corona between 1.4 and 10 $R_\odot$ with a field of view of 40′. In order to cover all possible position angles, the slit can be rotated by 360° about an axis pointing to the Sun's center. For a complete description of the UVCS instrument, see Kohl et al. (1995).

The lower limit of formation temperature of the O VI ions is $\sim 10^5$ K and the peak of the ionization fraction is at about 3.5×10^5 K (see Figure 1, taken from Giordano 1998 and obtained from the values given by Arnaud & Rothenflug 1985). These ions are therefore typically formed at the chromospheric level. In the inner solar corona, UV spectral lines are primarily generated by collisional excitation followed by radiative de-excitation. At higher levels, however, due to the strong, bright exciting chromospheric radiation, UV lines are also formed via resonant scattering of the O VI chromospheric radiation by the same coronal ions. In fact, as shown in Figure 1, the high temperature tail of the O VI's ionization fraction function persists up to a few 10^6 K, so that there is still an appreciable amount of O VI ions in the corona that are able to resonantly scatter the chromospheric radiation from the same ions. At a distance of 1.6 $R_\odot$, both the radiative and the collisional components are expected to contribute to the observed spectral line intensity.

Thus far, an unprecedented record of the distribution of the O VI intensity as a function of time, latitude, and longitude has been gathered by UVCS, covering a full solar cycle. The extended time interval of observation and the high latitude resolution ($\sim 3°$) are both pivotal in recognizing the expected patterns of periodicity due to the coronal differential rotation. The longitude resolution is only limited by the one-day data sampling, so that the minimum detectable separation of structures is about two days of solar rotation as viewed from the Earth, or $\sim 26°$ in longitude. Our investigation is focused on the period of maximum of solar activity. More precisely, we selected a four-year observation time interval, shown in Figure 2 as a shaded region, spanning from 1999 March 18 to 2002 December 31. In the time interval of interest for this work, UVCS has been running a counterclockwise daily synoptic observation program which covered the full corona from 1.6 to 3.0 $R_\odot$ at eight different roll angles separated by an angular step of 45°. Ancillary *special* observations have also been included in our study whenever the pointing was the same as the synoptic program. On average, the cadence of the data was about one per day, though unevenly spaced in time, with only a small number of gaps due to telemetry problems or special spacecraft maneuvers.

In this study, we will consider only data observed with the slit positioned at a projected distance of 1.6 $R_\odot$ from the

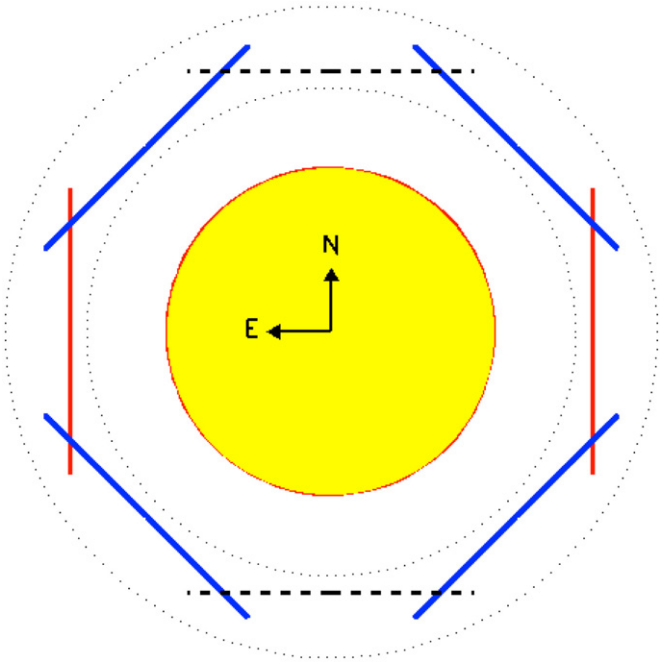

Figure 3. Sketch of the UVCS synoptic observation plan at 1.6 $R_\odot$, which is the lowest observed height in the time interval from 1999 to 2002. Red and blue straight lines display the UVCS slit positions relative to the Sun corresponding, respectively, to the equatorial and mid-latitude observations analyzed in this work. Polar observations (dashed lines) have only been used to build up the synoptic maps.

Sun center over mid-latitude (45°, 135°, 225°, and 315°) and equatorial regions (90° and 270°). The height of 1.6 $R_\odot$ was selected because it represents the lowest height reached by the synoptic observation program during the examined time span. An outline of the pointing of the UVCS synoptic observations used for this study is shown schematically in Figure 3. The raw UVCS data for the time interval of interest are available online from the SOLAR archive (Cora et al. 2003) at the INAF/OATo Web site http://solar.oato.inaf.it/. The data have been calibrated by using the most recent release of the UVCS Display and Analysis Software (version 40, available at the UVCS Web site http://cfa-www.harvard.edu/uvcs/), which also takes into account the time variations of the instrument performances. All the subsequent exposures with the same mirror pointing were summed up together, so that an average element of the time series is about 400 s long. For each selected roll angle, we used data acquired in a ±850 arcsec range around the center of the slit and, in order to increase the statistics, we further binned the data to 21 spatial elements along the slit for each observation, thus reducing the spatial resolution along the slit to 81 arcsec, corresponding to ∼3° in latitude at 1.6 $R_\odot$. The average daily time coverage is about 87%, spanning from 80% in the years 1999 and 2000, to 93% in 2001, and 96% in 2002. By averaging over the different roll angles, a set of 1208 data is thus available out of 1385 days of observations. Because of a *cross talk* effect among the two UVCS gratings and the mirror mechanisms, the effective observed heliocentric distances can be somewhat different by a few percent with respect to the nominal mirror pointings and may be further subject to changes over time. In fact, we verified that, in the time interval considered for this work, the 1.6 $R_\odot$ nominal pointing corresponds to actual mirror heights ranging from 1.50 to 1.57 $R_\odot$. Moreover, we emphasize that the projected distances of coronal features observed at the slit edges are located 0.21 $R_\odot$ higher (with respect to the Sun center) than at the slit center. Therefore, for a nominal mirror pointing at 1.6 $R_\odot$, the actual observed distance ranges from 1.50 $R_\odot$ at the slit center to as much as 1.78 $R_\odot$ at the slit edges. Altogether, the above effects should not represent a major problem in our analysis since, according to our previous results, we do not expect strong gradients of coronal rotation over the radial direction.

In order to estimate the total intensity of a selected spectral line from each coronal region element, the calibrated and combined UVCS spectra were fitted with a function resulting from the convolution of a Gaussian function, describing the coronal spectral profile, a Voigt curve, representing the instrumental broadening, and a function accounting for the slit width (Giordano 1998). All the data collected in the time interval under study were used to build up the O VI1032 Å intensity synoptic map at 1.6 $R_\odot$ shown in the upper panel of Figure 4. The lower panels further display yearly maps, from 1999 to 2002, that indeed show clear modulations which can be readily attributed to persistent coronal structures reappearing through several consecutive rotations. The brightest recurring coronal features are visible at mid-latitudes, while the modulation appears to be less pronounced in the equatorial region. With respect to the analysis performed in Paper I, where the coronal differential rotation was studied up to 45° of latitude from the equator (above which the signal-to-noise ratio was found to be too low for a reliable coronal rotation period determination), the present analysis extends up to about 75° from the solar equator. This is due to both the enhanced O VI coronal emission at solar maximum, as can be readily verified by comparing the intensity maps shown in Figure 4 with the analogous ones displayed in Figure 2 of Paper I, and the spread of solar activity over a wider range of latitudes.

A number of outliers in our time series data have been found to be clearly associated with emission from coronal mass ejections (CMEs) that are able to locally enhance the observed coronal UV (and specifically, O VI) intensity up to many factors for several tens of minutes (e.g., Raymond 2002; Mancuso et al. 2002; Ciaravella et al. 2006; Mancuso & Avetta 2008). During solar maximum activity, the daily CME rate has been estimated at about five per day, while at solar minimum it reduces to less than one (Gopalswamy et al. 2009). These transient events span almost all latitudes and last a few hours on average when observed in white light with coronagraphs such as the Large Angle and Spectrometric COronagraph (LASCO; Brueckner et al. 1995) instrument on board *SOHO*. Overall, CME detections tend to add biased noise (toward higher intensities) to the O VI intensity time series and represent therefore a known source of error. In order to evaluate the impact of CMEs on the observed intensity time series, we used the UVCS CME catalog recently embedded into the LASCO CME catalog (see http://cdaw.gsfc.nasa.gov/CME_list/). Over the four years covered by this study, the catalog contains 534 events detected by UVCS at different polar angles and heliocentric distances. Of these, only 85 CMEs have been observed at 1.6 $R_\odot$ over the six analyzed roll angles, meaning that, on average, in each one-year time series we expect no more than three or four CMEs. Therefore, the influence of these short lifetime events on the determination of the coronal rotation period is altogether negligible. On the other hand, studies on the rotation rate of the white-light corona (e.g., Nash 1991) have shown that CMEs have virtually no detectable effect on the coronal rotation rate. Anyway, in order to avoid unnecessary complications, CME-related outliers whose local contribution

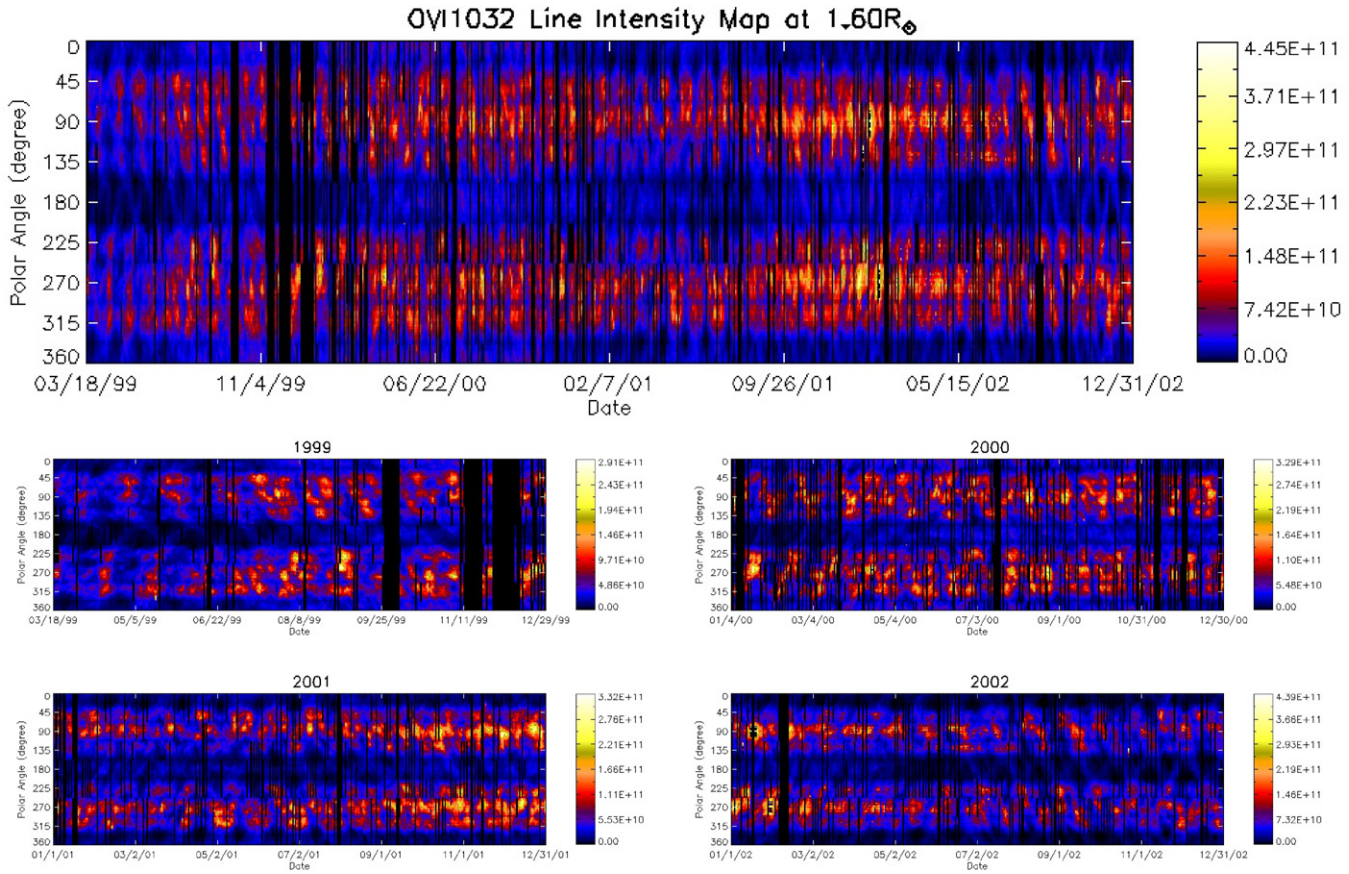

Figure 4. Upper panel: O VI 1032 Å intensity synoptic map at 1.6 $R_{\odot}$ in the time interval from 1999 March to 2002 December, corresponding approximately to Carrington rotations from CR 1947 to 1997. Lower panels: O VI 1032 Å intensity synoptic maps for each single year. Intensities are measured in units of photons cm^{-2} s^{-1} sr^{-1}. Position angles, measured counterclockwise (i.e., N–E–S–W–N) from the north pole, increase from top to bottom and cover all latitudes from 0° to 360°.

to the observed O VI intensity was 3σ above the mean were selectively removed from the O VI intensity time series.

3. PERIODICITY ANALYSIS

Our analysis is restricted to periodicities on timescales near the 27 day solar rotation period. We will initially consider one-year time series, since they represent a satisfactory compromise between time resolution, accuracy, and request of stationarity, and also allow direct comparison with the results from Paper I. The one-year window will then be shifted by monthly steps along the full four-year time span under study in order to detect possible long-term variations in the coronal differential rotation. In Paper I, two specific methods, the Lomb–Scargle periodogram (LSP; Lomb 1976; Scargle 1982) and the autocorrelation function (ACF), have been applied in order to retrieve the characteristic periods of coronal rotation during solar minimum conditions. In that work, the LSP method was mainly adopted because of its ability to deal with unevenly spaced data. At solar minimum, Giordano & Mancuso (2008) found a satisfactory agreement, within the quoted errors, between the results of the two different techniques. In the present work, however, a similar LSP analysis yielded unrealistic results and was therefore rejected. In order to double-check the results obtained with the classical ACF method, in this work we replaced the LSP method with a *discrete* version of the ACF technique (DACF; Edelson & Krolik 1988) that is able to retrieve the level of autocorrelation in unevenly sampled data sets without any interpolation or addition of artificial data points.

3.1. Autocorrelation Function (ACF)

The autocorrelation technique has been extensively applied in studies of coronal rotation (e.g., Parker et al. 1982; Fisher & Sime 1984; Parker 1986; Sime et al. 1989; Lewis et al. 1999; Lewis & Simnett 2001; Vats et al. 2001; Giordano & Mancuso 2008; Chandra et al. 2009). Although this time domain technique is often considered less powerful with respect to more sophisticated and higher resolution methods that operate in the frequency domain, it does avoid some of the problems that affect Fourier analysis techniques (such as aliasing), while allowing for a straightforward identification of the main periodicity in the signal. Of course, the detection of more than one periodicity is precluded by this technique and this fact does represent a strong limitation whenever multiple rotation periods are suspected in the same set of data. Since our latitude resolution is quite high, it is however reasonably improbable for two or more different rotation periods to be simultaneously present in the same one-year time series unless a time dependence of order a few months is suspected.

Briefly, the ACF measures the degree of linear correlation between a time series and the same time series lagged by a specified time interval. This function peaks at integer multiples of the period required for a particular feature to return to the same limb in subsequent rotations. Besides detrending, that is, removing a linear (or higher order) fit to the data, the standard autocorrelation procedure requires evenly sampled data. Since the set of N observations per year was unevenly distributed in time, the time series data were resampled at N equispaced intervals

by linear interpolation from neighboring values. Resampling of unevenly spaced data introduces a source of uncertainty in the rotation period estimation by ACF techniques, although, as already mentioned, we have approximately one measurement per day and rarely more than one measurement in a single day. At each latitude, estimates of the centroids of the individual (Nth) autocorrelation peaks were used to determine the coronal rotation period by dividing the lag at which they occurred by N. Error estimates for the ACF peaks were evaluated as the square root of the estimated variance of the ACF computed at the lags at which the peaks occurred. The estimation method (Bartlett 1946) is based on a general asymptotic expression for the variance of the sample autocorrelation coefficient of a stationary time series with independent, identically distributed normal errors. If a series is completely random, then, for a large sample of size N, the lagged-correlation coefficient is approximately normally distributed with mean 0 and variance $1/N$. The 95% confidence limits for the correlogram can therefore be plotted at $\pm 2/\sqrt{N}$. Only rotation period estimates corresponding to those peaks in the ACFs whose amplitudes were higher than the above confidence limit were considered. In general, for the whole yearly sets, only the first two or three peaks of the ACF satisfied this requirement for both limbs. Finally, the weighted averages of these semi-independent estimates, obtained from the autocorrelation analysis at the two limbs, were taken (at each latitude) as the rotation period. In determining the weighted mean of our estimates, weights were assigned equal to the inverse of the estimated variances of the ACF peaks. Statistical errors of the rotation periods were simply inferred by weighted standard deviation estimates.

3.2. Discrete Autocorrelation Function (DACF)

As already mentioned in the previous section, one important limitation of the ACF algorithm is that it requires evenly spaced time series and that it does not tolerate missing values. The discrete autocorrelation function (DACF), a technique first introduced by Edelson & Krolik (1988) and often used in astronomy for correlation analysis of sets of unevenly distributed data, adopts a binning scheme to overcome this problem. The main idea of the DACF technique is to bin the timescales suitably in the time coordinates of the ACF and calculate separately the mean correlation for each bin. This allows us to study the level of autocorrelation in unevenly sampled data sets without any interpolation or addition of artificial data points.

In practice, all pairs of data (y_i, y_j) of a discrete data set are first combined in unbinned discrete correlations:

$$\mathrm{UDACF}_{ij} = \frac{(y_i - \overline{y})(y_j - \overline{y})}{\sigma_y^2}, \qquad (1)$$

where $\overline{y}$ is the mean value of the data series and σ_y^2 is the corresponding standard deviation. The DACF for each time interval $\Delta t_{ij} = t_j - t_i$ is obtained by binning the UDACF_{ij} values in time for each time lag τ and averaging over the number of pairs whose time lag Δt_{ij} is in the range $\tau - \Delta\tau/2 \leqslant \Delta t_{ij} \leqslant \tau + \Delta\tau/2$. For further details, see also Hufnagel & Bregman (1992) and Ciprini et al. (2007).

4. ANALYSIS AND RESULTS

As in Paper I, the rotation period analysis was performed on the logarithms of the data in order to compress their dynamic range and reduce the impulsive effects on the time series due to the recurrence of active region streamers. This procedure allows us to obtain a more sinusoid-like signal (Weber et al. 1999) and to stabilize the data variance (Box & Cox 1964). In order to remove possible long-term variations, such as the intrinsic nonstationarity of the data linked to the intensity evolution of the corona along the solar cycle and trends due to the changing Sun–*SOHO* distance or uncorrected instrumental effects, each one-year time series was further detrended by subtracting a third-order polynomial fit to the original data. For each latitude within about 75° from the solar equator, we then derived the main significant coronal rotation periods estimated through the two autocorrelation techniques (ACF and DACF) discussed in the previous section.

The estimated coronal synodic rotation periods, together with their standard errors, are plotted with different symbols and displayed in Figure 5 as a function of heliographic colatitude (measured from the solar north pole). This figure shows the evolution of the differential coronal rotation rate with time obtained from the O VI coronal measurements at consecutive three-month intervals beginning from the time series centered on 1999 October and ending with the one centered on 2002 July. Overall, the results obtained from the application of the two autocorrelation techniques to the O VI intensity time series are in agreement, within the quoted errors, apart from a few exceptions. The reason why the DACF method yields essentially similar results with respect to the ACF method is that the data under analysis have been sampled with good regularity. The effect of unevenly distributed data on the estimate of periodicities in the O VI intensity time series obtained by UVCS is thus found to be of slight importance, in general, as already found in Paper I.

According to the results displayed in Figure 5, the coronal differentiality is observed to change quite smoothly during the full span of solar maximum activity, with a noticeable acceleration of the rotation rate with time close to the solar equator around the second part of the year 2000. Comparison with a similar coronal differential rotation profile obtained over a one-year time interval around solar minimum (see Paper I) suggests that the corona rotates less rigidly, although, strictly speaking, those data displayed only values up to ∼45° in latitude from the solar equator, so that a possible differentiality at higher latitudes, in the light of the present results, might have been hidden by the low signal-to-noise ratio affecting those data.

In order to extract more quantitative information on the time dependence of the equatorial coronal rotation rate, we computed a weighted mean of the results obtained around a ∼12° wide equatorial band. The resulting coronal synodic rotation periods as a function of time, together with their respective uncertainties, are displayed in Figure 6. A least-squares (Savitzky–Golay) polynomial smoothing filter has been further applied to the data, displayed as a solid line in the same figure. The plot clearly shows a decreasing trend from values compatible with the coronal synodic rotation period obtained at solar minimum (27.48 days; dashed line in Figure 6) near the end of the year 1999 to a weighted average of 25.7 days in the time interval extending from 2001 August to 2002 April, corresponding to as much as ∼7% acceleration of the equatorial rotation rate.

Mouradian et al. (2002), by analyzing the 10.7 cm radio emission flux covering cycles 19–22, established that the active corona rotation rate varies with respect to the 11 year sunspot cycle and that there is a relationship between rotation rate and magnetic flux, implying a positive correlation between solar activity and coronal rotation rate. Our results, however, when

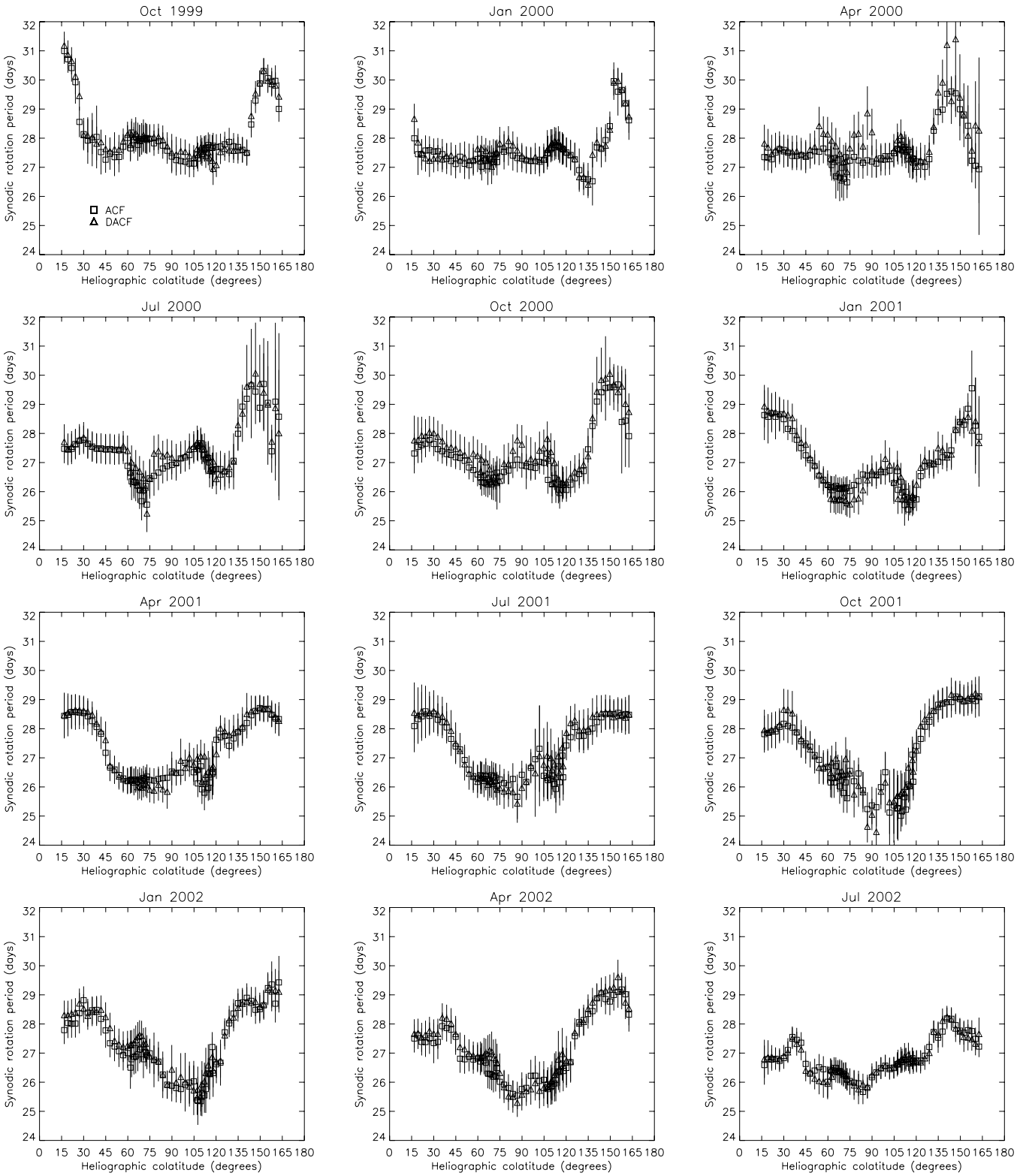

Figure 5. Colatitude dependence of the coronal rotation period obtained from the analysis of the O VI 1032 Å intensities at 1.6 $R_{\odot}$. A one-year window has been shifted by three months along the full four-year time span under study, starting from the time series centered on the month of 1999 October. Different symbols identify coronal rotation periods obtained through the periodicity analysis using the ACF (open squares) and DACF (open triangles) techniques.

compared with the estimates obtained in our previous work (Paper I) during solar minimum, do not seem to support the above conclusions.

A similar analysis was performed on data observed at a set of four latitudes taken at steps of 15° north and south of the solar equator. In this case, weighted averages of the coronal rotation periods obtained for both the northern and the southern hemispheres were considered. The results are plotted in Figure 7, together with their respective uncertainties and least-squares polynomial smoothing filters applied to the data. While the

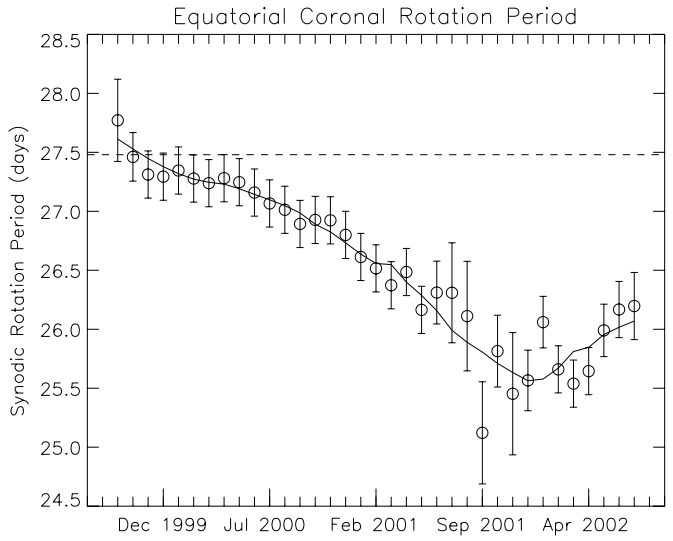

Figure 6. Equatorial coronal rotation period (open circles) as a function of time. The solid line shows a least-squares (Savitzky–Golay) polynomial smoothing filter applied to the data. The dashed line points out the equatorial rotation rate estimated by Giordano & Mancuso (2008) at solar minimum.

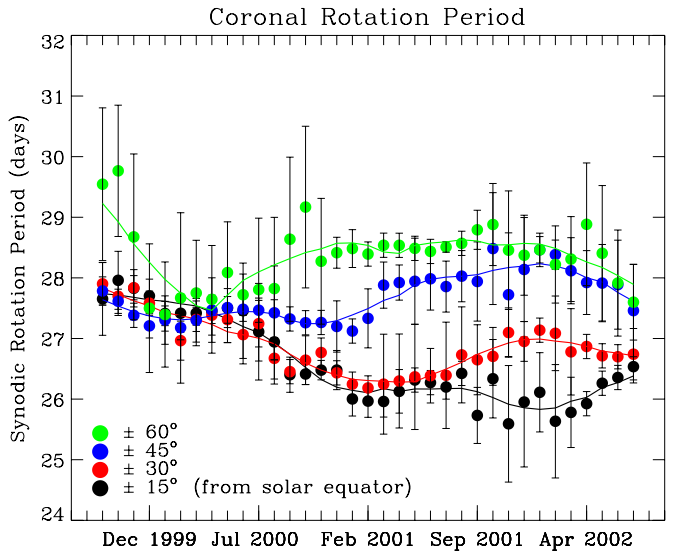

Figure 7. Coronal rotation rate at four different latitudes as a function of time. The solid lines show least-squares (Savitzky–Golay) polynomial smoothing filters applied to the data.

coronal rotation period as a function of time (obtained over a ∼12° wide latitude band located around 15° north and south of the solar equator) shows a similar trend to the one estimated around the equatorial band, some remarkable differences are noticeable at higher latitudes. In particular, around 30° north and south of the solar equator, although a decrease in the coronal rotation period is still noticeable, at least up to mid 2001, the coronal rotation period is seen to grow again around the year 2002, averaging to about 27 days. A completely different behavior is instead obtained for the coronal rotation period estimates beyond 45° in latitude from the solar equator, where the acceleration observed at lower latitudes is not present throughout the whole considered time interval.

The latitudinal rotation profile of the solar corona over the whole solar maximum activity of cycle 23, obtained by averaging the yearly results from both techniques over the four-year time interval, is shown in Figure 8, together with the estimated uncertainties. For comparison, we overplotted in the same figure the analytical approximations to typical differential rotation profiles of the photosphere (from Pierce & LoPresto 1984) and sunspots (from Nesme-Ribes et al. 1993) obtained during solar maximum conditions. From the above comparison, it is clear that the coronal magnetic structures tend to rotate much faster at all latitudes, and less differentially, than the underlying small-scale magnetic structures linked to the photospheric plasma. The rotation rate of sunspots is however compatible, at least within a band of ∼40° around the solar equator, with the one estimated in the middle corona.

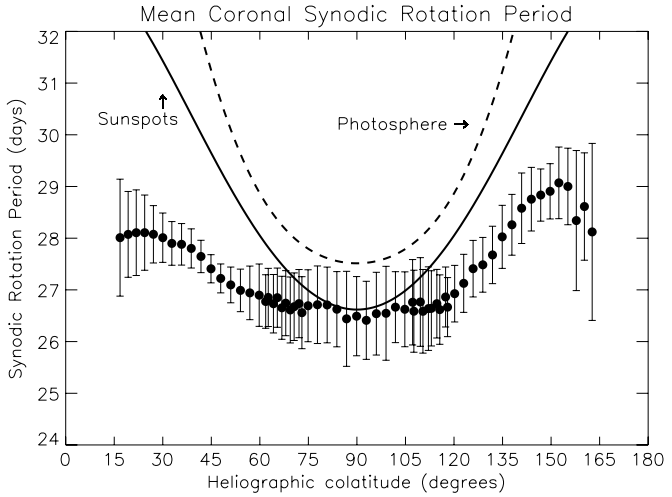

Figure 8. Colatitude dependence of the coronal synodic rotation period in days obtained by averaging the estimates from the two autocorrelation techniques of periodicity analysis over the epoch 1999–2002 (filled circles). The dashed and solid lines represent, respectively, analytical approximations to typical differential rotation profiles of the photosphere (Pierce & LoPresto 1984) and sunspots (Nesme-Ribes et al. 1993) obtained during solar maximum activity.

For completeness, we point out that the average coronal differential rotation profile at solar maximum displayed in Figure 8 is suggestive of a possible north–south asymmetry, as already noticed at solar minimum (see Paper I), with the northern hemisphere appearing to rotate somewhat faster than the southern hemisphere above ∼45° from the solar equator. The differences are however within the quoted errors at all latitudes.

5. CONCLUSIONS

Following a previous investigation by Giordano & Mancuso (2008) on the differential coronal rotation during solar minimum conditions as deduced from UVCS/*SOHO* observations of the O VI 1032 Å spectral line, we established the rotational characteristics of the solar corona at the maximum of solar activity in the time interval from 1999 March to 2002 December. The latitudinal range of the data considered for this work, retrieved at a nominal slit height of 1.6 $R_{\odot}$, extends from the solar equator up to ∼75° toward the poles, with enough spatial resolution to reveal the latitudinal dependence of the coronal rotation rate. Coronal synodic rotation periods as a function of colatitude and time were obtained by means of two methods, that is, the classical autocorrelation (ACF) technique and its *discrete* version (DACF), in order to double-check the results and retrieve the level of autocorrelation in unevenly sampled data sets without any interpolation or addition of artificial data points.

In our analysis, restricted to periodicities on timescales near the 27 day solar rotation period, we first considered the time series of the O VI intensity data in yearly pieces, determining the rotation rate versus colatitude within a one-year window that was shifted by monthly steps along the full four-year time span under study, thus allowing us to determine the long-term variation in the rotation of the solar corona at all the available latitudes. Finally, the data were combined to obtain the time-averaged coronal rotation rate during solar maximum conditions.

From the above analysis, it is shown that the coronal rotation differential profile tends to be less rigid, that is, more differential, during solar maximum activity. Although the estimated equatorial coronal synodic rotation period is initially consistent with the value found by Giordano & Mancuso (2008) around solar minimum (∼27.5 days), a systematic acceleration occurs in the second half of the year 2000, with the equatorial synodic rotation period settling to an average value of 25.7 days in the time interval extending from 2001 August to 2002 April, corresponding to as much as ∼7% acceleration of the coronal equatorial rotation rate.

The coronal rotation rate as a function of colatitude as determined over the whole time interval considered in this work also confirms the overall rigidity of the corona during periods of maximum activity with respect to the lower layers of the solar atmosphere. In general, the coronal magnetic structures tend to rotate much faster at all latitudes, and less differentially, than the underlying small-scale magnetic structures linked to the photospheric plasma. The rotation rate of sunspots is however found to be compatible, at least within a band of ∼40° around the solar equator, with the one estimated in the middle corona.

Finally, although the average coronal differential rotation profile at solar maximum is suggestive of a possible north–south asymmetry, as already noticed at solar minimum, with the northern hemisphere appearing to rotate somewhat faster than the southern hemisphere above ∼45° from the solar equator, the differences are within the quoted errors at all latitudes.

This research has been supported by contract ASI/I/035/05/0 of the Italian Space Agency (ASI). *SOHO* is a project of international cooperation between European Space Agency (ESA) and National Aeronautics and Space Administration (NASA). UVCS is a joint project of NASA, ASI, and Swiss Funding Agencies.

REFERENCES

Altrock, R. C. 2003, Sol. Phys., 216, 343
Arnaud, M., & Rothenflug, R. 1985, A&AS, 60, 425
Aschwanden, M. J., Lim, J., Gary, D. E., & Klimchuk, J. A. 1995, ApJ, 454, 512
Bartlett, M. S. 1946, J. R. Stat. Soc. Suppl., 8, 27
Box, G. E. P., & Cox, D. R. 1964, J. R. Statistical Soc. Ser. B, 26, 211
Brueckner, G. E., et al. 1995, Sol. Phys., 162, 357
Chandra, S., Vats, H. O., & Iyer, K. N. 2009, MNRAS, 400, L34
Ciaravella, A., Raymond, J. C., & Kahler, S. W. 2006, ApJ, 652, 774
Ciprini, S., Takalo, L. O., Tosti, G., Raiteri, C. M., Fiorucci, M., Villata, M., Nucciarelli, G., Lanteri, L., Nilsson, K., & Ros, J. A. 2007, A&A, 467, 465
Cora, A., Antonucci, E., Dimitoglou, G., Volpicelli, C. A., & Giordano, S. 2003, Mem. Soc. Astron. Ital., 74, 819
Domingo, V., Fleck, B., & Poland, A. I. 1995, Sol. Phys., 162, 1
Edelson, R. A., & Krolik, J. H. 1988, ApJ, 333, 646
Fisher, R. R., & Sime, D. G. 1984, ApJ, 287, 959
Giordano, S. 1998, PhD thesis, Univ. Torino
Giordano, S., & Mancuso, S. 2008, ApJ, 688, 656 (Paper I)
Gopalswamy, N., Yashiro, S., Michalek, G., Stenborg, G., Vourlidas, A., Freeland, S., & Howard, R. 2009, Earth Moon Planets, 104, 295
Hansen, R. T., Hansen, S. F., & Loomis, H. G. 1969, Sol. Phys., 10, 135
Hoeksema, J. T., & Scherrer, P. H. 1987, ApJ, 318, 428
Hufnagel, B. R., & Bregman, J. N. 1992, ApJ, 386, 473
Kohl, J. L., et al. 1995, Sol. Phys., 162, 313
Lewis, D. J., & Simnett, G. M. 2001, Sol. Phys., 200, 75
Lewis, D. J., Simnett, G. M., Brueckner, G. E., Howard, R. A., Lamy, P. L., & Schwenn, R. 1999, Sol. Phys., 184, 297
Lomb, N. R. 1976, Ap&SS, 39, 447
Mancuso, S., & Avetta, D. 2008, ApJ, 677, 683
Mancuso, S., Raymond, J. C., Kohl, J., Ko, Y.-K., Uzzo, M., & Wu, R. 2002, A&A, 383, 267
Mouradian, Z., Bocchia, R., & Botton, C. 2002, A&A, 394, 1103
Nash, A. G. 1991, ApJ, 366, 592
Nesme-Ribes, E., Ferreira, E. N., & Mein, P. 1993, A&A, 274, 563
Parker, G. D. 1986, Sol. Phys., 104, 333
Parker, G. D., Hansen, R. T., & Hansen, S. F. 1982, Sol. Phys., 80, 185
Pierce, A. K., & Lopresto, J. C. 1984, Sol. Phys., 93, 155
Raymond, J. C. 2002, in From Solar Min to Max: Half a Solar Cycle with *SOHO*, ed. A. Wilson (ESA SP-508; Noordwijk: ESA), 421
Rybak, J. 1994, Sol. Phys., 152, 161
Scargle, J. D. 1982, ApJ, 263, 835
Sime, D. G., Fisher, R. R., & Altrock, R. C. 1989, ApJ, 336, 454
Timothy, A. F., Krieger, A. S., & Vaiana, G. S. 1975, Sol. Phys., 42, 135
Tlatov, A. G. 2006, Astron. Rep., 50, 325
Vats, H. O., Cecatto, J. R., Mehta, M., Sawant, H. S., & Neri, J. A. C. F. 2001, ApJ, 548, L87
Wang, Y.-M., Sheeley, N. R., Jr., Nash, A. G., & Shampine, L. R. 1988, ApJ, 327, 427
Wang, Y.-M., et al. 1997, ApJ, 485, 419
Weber, M. A., Acton, L. W., Alexander, D., Kubo, S., & Hara, H. 1999, Sol. Phys., 189, 271